

RESEARCH PAPER



LncRNA RP3-326113.1 promotes cisplatin resistance in lung adenocarcinoma by binding to HSP90B and upregulating MMP13

Huixin Zhou^{a*}, Xiaolu Huang^{a*}, Wenjing Shi^{a*}, Shihao Xu^b, Jie Chen^c, Kate Huang^d, and Yumin Wang^a

^aDepartment of Laboratory Medicine, The First Affiliated Hospital of Wenzhou Medical University, Wenzhou, P.R. China; ^bDepartment of Ultrasound Imaging, The First Affiliated Hospital of Wenzhou Medical University, Wenzhou, P.R. China; ^cDepartment of Intensive Care Unit, The First Affiliated Hospital of Wenzhou Medical University, Wenzhou, P.R. China; ^dDepartment of Pathology, The First Affiliated Hospital of Wenzhou Medical University, Wenzhou, P.R. China

ABSTRACT

Cisplatin (DDP) resistance has become the major obstacle in the therapy of malignant tumors, including lung adenocarcinoma (LAD). Long non-coding RNAs (lncRNAs) were confirmed to be related to DDP-resistance. Studies have shown that RP3-326113.1 (also known as PINCR) could promote the progression of colorectal cancer, and RP3-326113.1 knockdown could induce hypersensitivity to chemotherapy drugs. While the function of RP3-326113.1 in LAD is unclear, therefore, this study aimed to research the biological function and related molecular mechanisms of RP3-326113.1 in DDP-resistance of LAD. QPCR analysis found that RP3-326113.1 was highly expressed in A549/DDP cells and LAD tissues. Cytological assays found that RP3-326113.1 promoted the proliferation, migration, invasion, and DDP-resistance of LAD cell lines. Moreover, knock-down of RP3-326113.1 could induce G1 phase arrest. Nude mouse xenograft assay confirmed that RP3-326113.1 could promote tumor growth and DDP-resistance in vivo. Mechanically, RNA pull-down and mass spectrometry analysis indicated that heat shock protein HSP 90-beta (HSP90B) could be combined with RP3-326113.1. HSP90B knockdown inhibited the effect of RP3-326113.1 on proliferation, invasion, and promoted LAD cell lines apoptosis. Transcriptome sequencing analysis found that MMP13 was the downstream mRNA of RP3-326113.1. In conclusion, RP3-326113.1 could promote DDP-resistance of LAD by binding to HSP90B and upregulating human matrix metalloproteinase-13 (MMP-13) and may serve as a therapeutic target, as well as a biomarker for predicting DDP-resistance in LAD.

Abbreviations:

DDP: Cisplatin; LAD: Lung adenocarcinoma; lncRNAs: Long non-coding RNAs; qPCR: real-time fluorescent quantitative PCR; HSP90B: Heat shock protein HSP 90-beta; RPMI: Roswell Park Memorial Institute; FBS: Fetal bovine serum; CT: computed tomography; MRI: magnetic resonance imaging; RECIST: Response evaluation criteria in solid tumors; NC: Negative control; OE: over-expression; shRNA: short hairpin RNA; siRNA: small interfering RNA; CCK-8: Cell Counting Kit-8; IC50: The half maximal inhibitory concentration; PBS: Phosphate buffer saline; PI: propidium iodide; SDS-PAGE: sodium dodecylsulfate-polyacrylamide gel electrophoresis; ceRNA: Competing endogenous RNA; HE: hematoxylin-eosin; ns: no significance.

ARTICLE HISTORY

Received 11 November 2021
Revised 30 January 2022
Accepted 7 March 2022



KEYWORDS

Lung adenocarcinoma;
cisplatin resistance; RP3-326113.1

Introduction

Lung adenocarcinoma (LAD) is a common type of lung cancer [1]. For operable LAD, postoperative adjuvant chemotherapy could improve the survival rate of patients [2]. The first-line treatment scheme is a combination of cisplatin (DDP)-based drugs, which has been used as the standard adjuvant treatment scheme in advanced stages [3,4]. However, the emergence of DDP-

resistance seriously affected the prognosis of patients [5]. The mechanisms of DDP-resistance mainly include abnormal DNA damage repair function, intracellular drug inactivation, and changes of drug resistance-related genes and so on [6,7]. Therefore, finding new ways to regain the sensitivity of LAD-resistant cells to DDP is of great significance for improving patients' outcomes.

CONTACT Kate Huang  kate0577@163.com  Department of Pathology, The First Affiliated Hospital of Wenzhou Medical University, Nanbaixiang Street, Wenzhou 325000, P.R. China; Yumin Wang  wangyumin0577@wmu.edu.cn  Department of Laboratory Medicine, The First Affiliated Hospital of Wenzhou Medical University, Nanbaixiang Street, Wenzhou 325000, P.R. China

*These authors contributed equally to this work.

Long non-coding RNAs (lncRNAs) lack protein-coding functions but can exert their function in epigenetics, transcription, and post-transcription through interactions between DNA, RNA, and proteins [8–10]. Increasing studies have indicated that lncRNAs are involved in the promotion of tumor occurrence, metastasis, and resistance to chemotherapy [11–13]. Our pre-experimental found that lncRNA RP3-326I13.1 (also known as lncRNA PINCR) was overexpressed in colon cancer and was responding to the DNA damage through the p53/PINCR/Matrin3 axis [14].

Heat shock protein 90 (Hsp90) is a molecular chaperone that can participate in a variety of cellular processes including DNA repair, development, transport, and protein degradation [15,16], and plays an important role in the occurrence and development of tumors. Among them, HSP90B could interact with Microtubule-associated serine/threonine kinase 1 (MAST1) to block the ubiquitination of MAST1 at lysines 317 and 545, and prevent proteasome degradation, thereby enhancing MAST1-mediated DDP-resistance [17].

In this study, we used gene chip and real-time quantitative PCR (qPCR), cell culture, animal experiment, and so on, to thoroughly study the biological function and molecular mechanism of lncRNA RP3-326I13.1 promotes cisplatin resistance in lung adenocarcinoma.

Results

RP3-326I13.1 was highly expressed in DDP-resistant LAD tissues and cells

To study the role of lncRNAs in DDP-resistance of LAD, we compared the differential genes in DDP-sensitive A549 cells and DDP-resistant A549/DDP cells through gene chip, and found that RP3-326I13.1 was significantly increased in A549/DDP (change fold = 121.053) (Figure 1(a)). We subsequently verified it in cells and tissues by qPCR and found that RP3-326I13.1 was highly expressed in DDP-resistant A549/DDP cells and 57 cases LAD tissues (Figure 1(b,c)). In addition, compared with DDP-sensitive tissues with disease relief, RP3-326I13.1 expression was higher in DDP-resistant tissues with disease progression (Figure 1(d)).

Compared with A549 cells, the IC₅₀ value of DDP enhanced in A549/DDP cells, demonstrating that A549/DDP cells had high DDP-resistance (Figure 1(e)).

RP3-326I13.1 enhanced DDP-resistance by promoting the proliferation, migration, and invasion of LAD cell lines

Since RP3-326I13.1 was high expression in A549/DDP and low expression in A549 cells, we chose to overexpress RP3-326I13.1 in A549 cells, and knock down RP3-326I13.1 in A549/DDP cells to verify the function of RP3-326I13.1 in DDP-resistance. QPCR results confirmed that we successfully constructed the OE-RP3-326I13.1 A549 cells and sh-RP3-326I13.1 A549/DDP cells (Figure 2(a,b)). Then, we found that RP3-326I13.1 overexpression increased the IC₅₀ value of DDP in A549 cells, while RP3-326I13.1 knockdown significantly decreased the IC₅₀ value of DDP in A549/DDP cells (Figure 2(c)).

CCK-8 assays showed that the OE-RP3-326I13.1 group promoted the proliferation of LAD cell lines, after treatment with DDP (1 µg/ml), the cell proliferation was inhibited, but RP3-326I13.1 overexpression reversed the inhibitory effect of DDP in A549 cells (Figure 2(d)). Sh-RP3-326I13.1 group inhibited the proliferation of A549/DDP cells and the cells proliferation was inhibited after treatment with DDP (2 µg/ml) (Figure 2(e)). We found that the OE-RP3-326I13.1 group promoted clone formation ability, and it was inhibited after treatment with DDP, while RP3-326I13.1 knockdown group had the opposite effect (Figure 2(f)).

Cell cycle assays found that the proportion of G2 + S phase cells increased after RP3-326I13.1 overexpression, but the proportion of G1 phase cells also increased. There was no significant difference in the G1 and G2 + S phase after treatment with DDP (Figure 2(g)). RP3-326I13.1 knockdown increased the proportion of G1 phase cells, and the proportion of G2 + S phase cells decreased accordingly. After DDP interference, G1 phase cells increased, and G2 + S phase cells decreased correspondingly, and RP3-326I13.1 knockdown further strengthened this phenomenon (Figure 2(g)). We found that the OE-RP3-326I13.1 group promoted

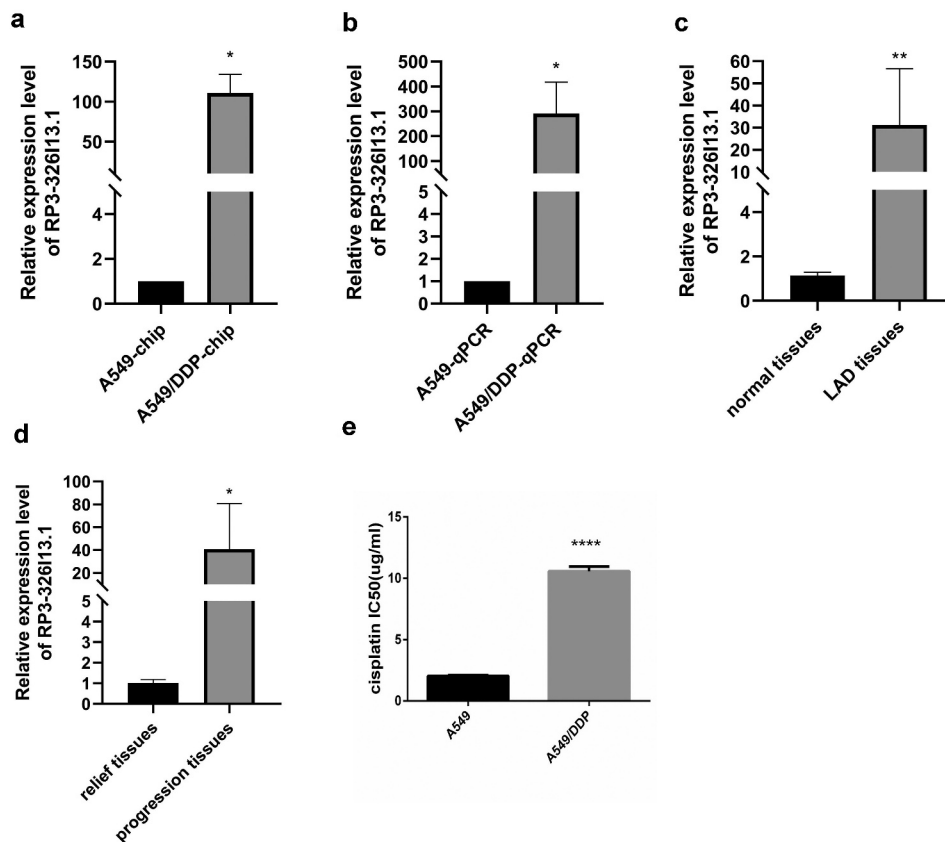


Figure 1. RP3-326113.1 was highly expressed in cisplatin (DDP) resistant lung adenocarcinoma (LAD) tissues and cells. (a) LncRNAs gene chip was used to detect RP3-326113.1 expression in A549 cells and A549/DDP cells and found that RP3-326113.1 was significantly increased in A549/DDP. (b) We found that RP3-326113.1 was highly expressed in DDP-resistant A549/DDP cells. (c) Mann-Whitney U test shown that the expression level of RP3-326113.1 in LAD tissues ($n = 57$) was significantly higher than that in adjacent tissues ($n = 57$). (d) Mann-Whitney U test shown that the expression level of RP3-326113.1 in the tissues of patients with progressive LAD (cisplatin treatment-naïve) ($n = 32$) was significantly higher than that of patients in complete remission ($n = 25$). (e) Compared with A549 cells, the IC₅₀ value of DDP enhanced in A549/DDP cells. Cytological experiments were repeated three times and their statistics were performed using t-test. * $P < 0.05$, ** $P < 0.01$, **** $P < 0.0001$.

the migration and invasion of LAD cell lines. After treatment with DDP, the migration and invasion ability were significantly lower than those untreated with DDP, but RP3-326113.1 overexpression reversed the inhibitory effect of DDP, RP3-326113.1 knockdown cells produced the opposite results (Figure 2(h-j)).

HSP90B cooperates with RP3-326113.1 to promote DDP-resistance of LAD

PCR amplified the sense and antisense strands of RP3-326113.1 to obtain an in vitro transcribed DNA template of the A549 cells. The electrophoresis diagram of the PCR products was shown in Figure 3(a). Then, we performed RNA pulldown, and silver staining to detect the proteins bound to RP3-326113.1 (Figure 3(b)), there were no obvious

difference bands. Subsequently, we performed mass spectrometry identification and obtained the Venn diagram of the differential proteins (Figure 3(c)). The protein-related information with obvious differences is shown in Table 1, and HSP90B has been reported to be involved in DDP-resistance [17]. In addition, we used the RNA-Protein Interaction Prediction website (<http://pridb.gdcb.iastate.edu/RPISeq/>) [18] to find that there was a strong interaction between HSP90B and the 3'-UTR of RP3-326113.1 (interaction probability > 0.8) (Figure 3(d)). Therefore, according to the above results, we chose HSP90B for the next study.

We found that HSP90B was highly expressed in A549/DDP cells, LAD tissues, and LAD progression tissues (Figure 3(e-g)). Subsequently, we knocked down HSP90B expression in A549/DDP

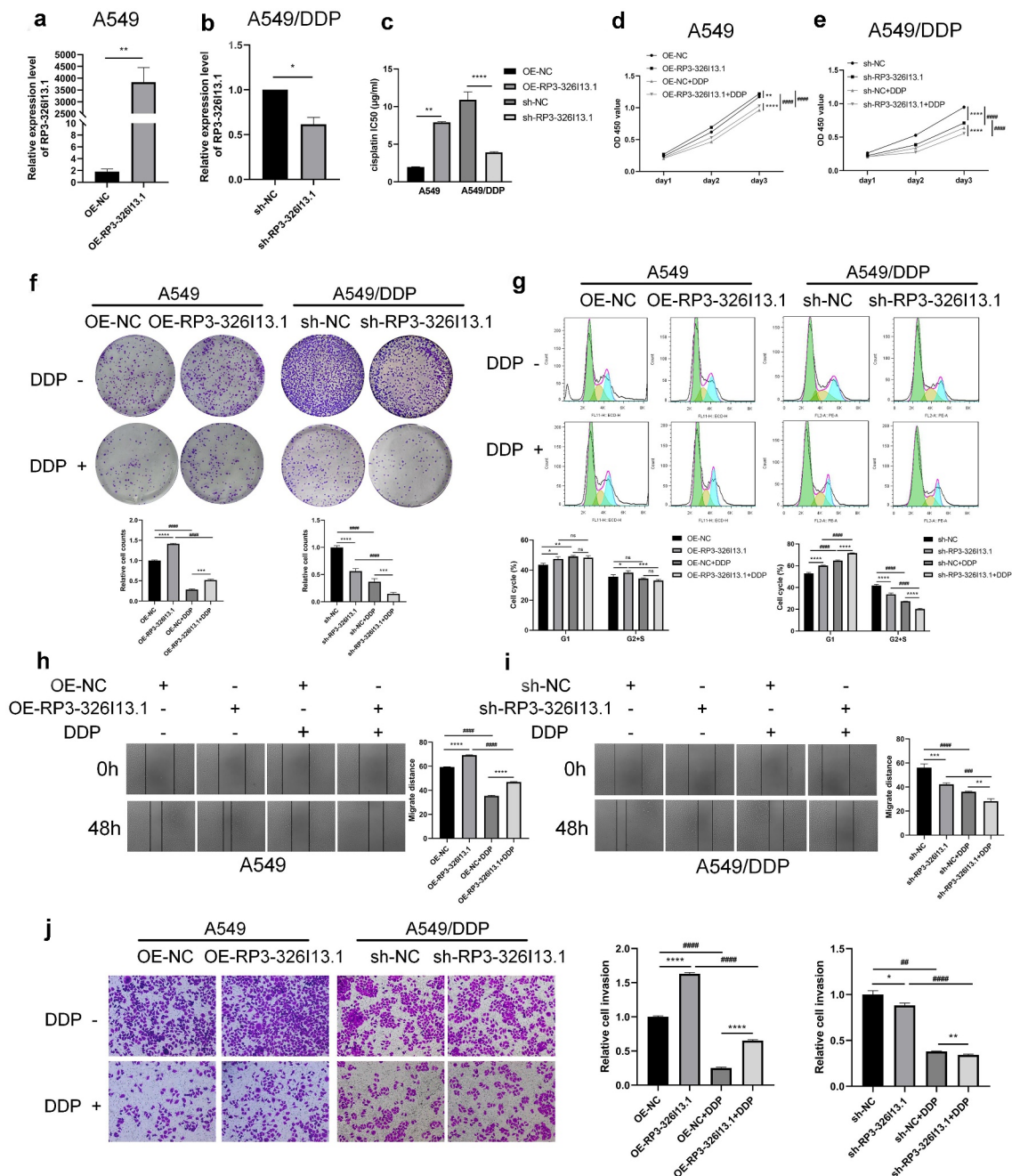


Figure 2. RP3-326113.1 was essential for proliferation, migration, invasion and DDP-resistance of LAD cell lines. (a) The expression level of RP3-326113.1 of the OE-RP3-326113.1 (RP3-326113.1 overexpression) A549 cell was higher than that of A549 OE NC cells. (b) The expression level of RP3-326113.1 of sh-RP3-326113.1 (RP3-326113.1 knockdown) A549/DDP cell decreased than sh-RP3-326113.1 NC A549/DDP cell. (c) We found that RP3-326113.1 overexpression increased the IC50 values of DDP in A549 cells, while RP3-326113.1 knockdown significantly decreased the IC50 values of DDP in A549/DDP cells. (d) CCK-8 assay showed that the OE-RP3-326113.1 group promoted LAD cell proliferation, which was inhibited by treatment with DDP (1 µg/ml), but RP3-326113.1 overexpression reversed the inhibitory effect of DDP in A549 cells. (e) Sh-RP3-326113.1 group inhibited the proliferation of LAD cell lines. After treatment with DDP (2 µg/ml), the proliferation of cells was inhibited. (f) We found that the OE-RP3-326113.1 group promoted clonogenic ability, which was inhibited by DDP treatment, while the opposite was true for the RP3-326113.1 knockdown group. (g) Cell cycle testing found that after RP3-326113.1 overexpression, the proportion of cells in G2 + S phase increased, but the proportion of cells in G1 phase also increased. After treatment with DDP, there is no significant difference between G1 and G2 + S phases. (h-j) OE-RP3-326113.1 group promoted the migration and invasion of LAD cell lines (200 times under the mirror). After treatment with DDP, migration and invasion were significantly lower than those without DDP treatment, but RP3-326113.1 overexpression reversed the inhibitory effect of DDP, and RP3-326113.1 knockdown cells produced the opposite result. Cytological experiments were repeated three times. * $P < 0.05$, ** $P < 0.01$, *** $P < 0.001$, **** $P < 0.0001$, ## $P < 0.01$, ### $P < 0.001$, #### $P < 0.0001$.

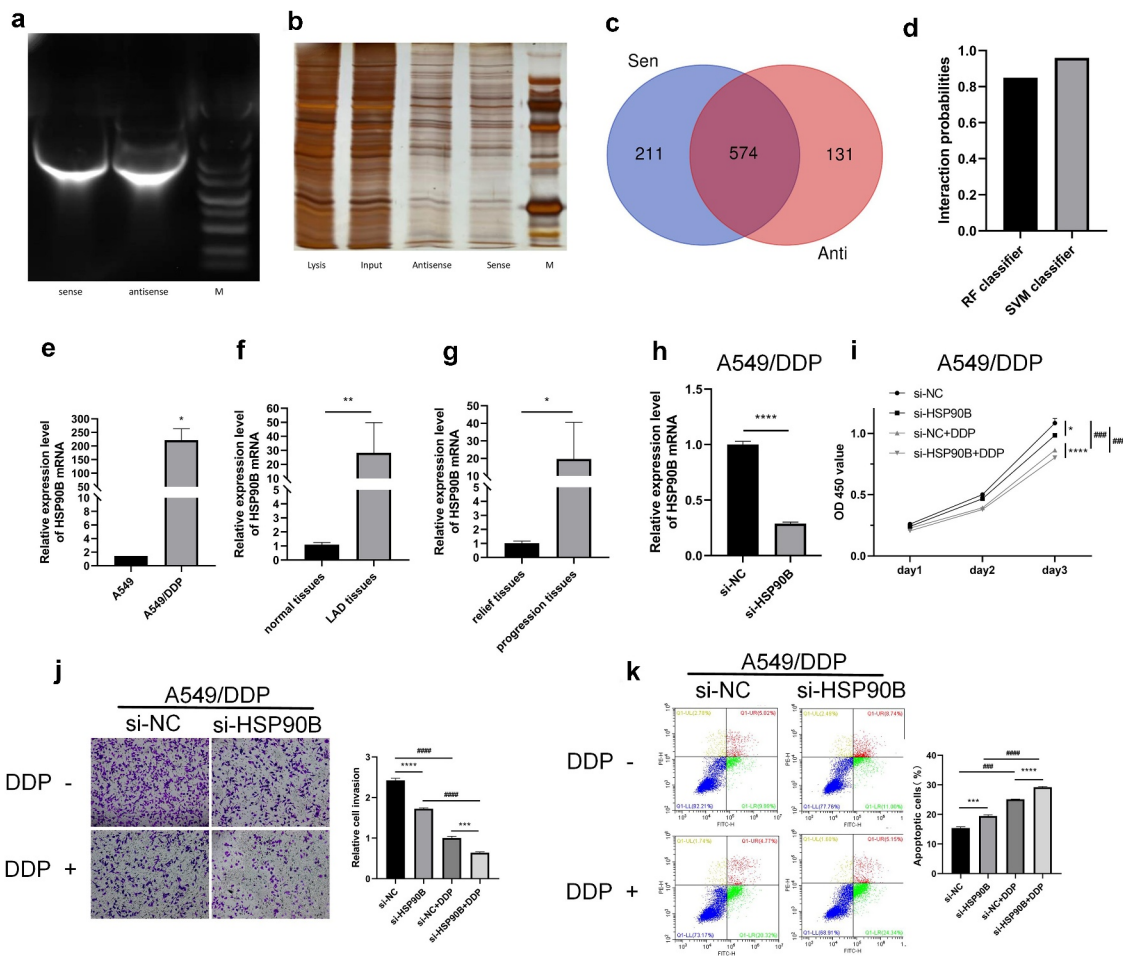


Figure 3. RP3-326I13.1 promoted LAD cell proliferation, invasion and DDP-resistance by combining with HSP90B. (a) It showed the electrophoresis diagram of the PCR products. (b) RNA pulldown and silver staining figure of RBP bound to RP3-326I13.1. (c) We carried out mass spectrometry identification and obtained Venn diagrams of different proteins. (d) Interaction potential between HSP90B and the 3'-UTR of RP3-326I13.1 was predicted by RNA-Protein Interaction Prediction. (e-g) RT-qPCR was used to detect HSP90B expression in A549 cells and A549/DDP cells, adjacent tissues and LAD tissues, relief tissues and progression tissues. (h) HSP90B expression was knocked down in A549/DDP cells. (i) Compared with the si-NC group, the si-HSP90B group can inhibit cell proliferation. After treatment with DDP, the cell proliferation is inhibited, and the si-HSP90B+DDP group has a stronger inhibitory effect on A549/DDP cells. (j) knockdown of HSP90B inhibited cell invasion, and was inhibited by treatment with DDP, and knockdown of HSP90B further inhibited invasion. (k) HSP90B knockout promoted apoptosis of A549/DDP cells, while DDP treatment produced more apoptotic cells. * $P < 0.05$, ** $P < 0.01$, *** $P < 0.001$, **** $P < 0.0001$, ### $P < 0.001$, #### $P < 0.0001$.

cells (Figure 3(h)). Compared with the si-NC group, the si-HSP90B group inhibited cell proliferation, and after treatment with DDP, the cell proliferation was inhibited, and the si-HSP90B+DDP group had stronger inhibitory effects in A549/DDP cells (Figure 3(i)), indicating that HSP90B knockdown could inhibit the proliferation and DDP-resistance of A549/DDP cells. We found that the HSP90B knockdown inhibited cell invasion, and after treatment with DDP, cell invasion was inhibited, and HSP90B knockdown further inhibit the invasion (Figure 3(j)). In addition, we found that HSP90B knockdown promoted

A549/DDP cells apoptosis, and DDP treatment caused more cells to undergo apoptosis (Figure 3(k)).

HSP90B knockdown could reverse the tumor-promoting effect of RP3-326I13.1

To further verify the relationship between RP3-326I13.1 and HSP90B, we co-transfected OE-RP3-326I13.1 and si-HSP90B vectors in A549 cells. CCK-8 results displayed that HSP90B knockdown successfully reversed the pro-proliferation effect of RP3-326I13.1 in both groups with or without DDP

Table 1. Clinical features of 57 lung adenocarcinoma patients.

Term	Case (n)
Sex	
Male	28
Female	29
TMN stage	
Ia	12
Ib	28
IIa	7
IIb	2
IIIa	8
Degree of tissue differentiation	
Poor	11
Poor-moderate	7
Moderate	17
Moderate-high	9
High	13
Lymph node metastasis	
Yes	14
No	43
Smoking	
Yes	20
No	37

treatment (Figure 4(a,b)). HSP90B knockdown reversed the pro-invasive effect of RP3-326I13.1

in both groups with or without DDP treatment (Figure 4(c,d)). Similarly, the apoptosis assays also found that HSP90B knockdown reversed the anti-apoptotic ability of RP3-326I13.1 and produced more apoptotic cells in both groups with or without DDP intervention (Figure 4(e,f)).

MMP13 served as a downstream mRNA of RP3-326I13.1

In the RP3-326I13.1 overexpression and knockdown groups, we obtained multiple differentially expressed mRNA through transcriptome sequencing (Figure 5(a)), including MMP13, CP, ICAM1, CDK18, PARP14, OAS3, CXCL8, and PLEKHA4. Further RT-QPCR results showed that MMP13, CP, ICAM1, CDK18, and OAS3 were all up-regulated in RP3-326I13.1 overexpression cells, and down-regulated in RP3-326I13.1 knockdown cells (Figure 5(b-i)).

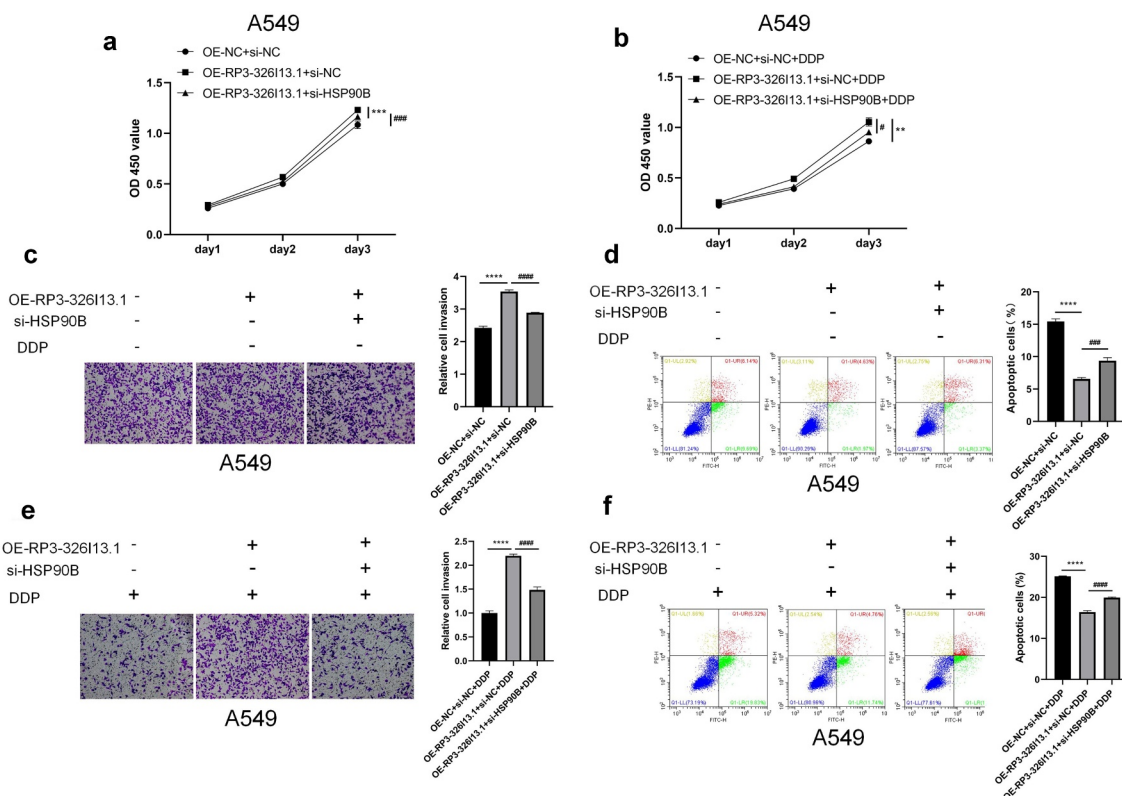


Figure 4. HSP90B knockdown could reverse the tumor-promoting effect of RP3-326I13.1. (a, b) HSP90B knockdown successfully reversed the pro-proliferative effect of RP3-326I13.1 in both groups with and without DDP treatment. (c, d) HSP90B knockdown reversed the pro-invasive effect of RP3-326I13.1 in both groups with and without DDP treatment. (e, f) Knockout of HSP90B reversed the anti-apoptotic ability of RP3-326I13.1 and produced more apoptotic cells in the two groups with or without DDP intervention. Invasion experiments were observed using 200 times under the mirror. ** $P < 0.01$, *** $P < 0.001$, **** $P < 0.0001$, # $P < 0.05$, ### $P < 0.001$, #### $P < 0.0001$.

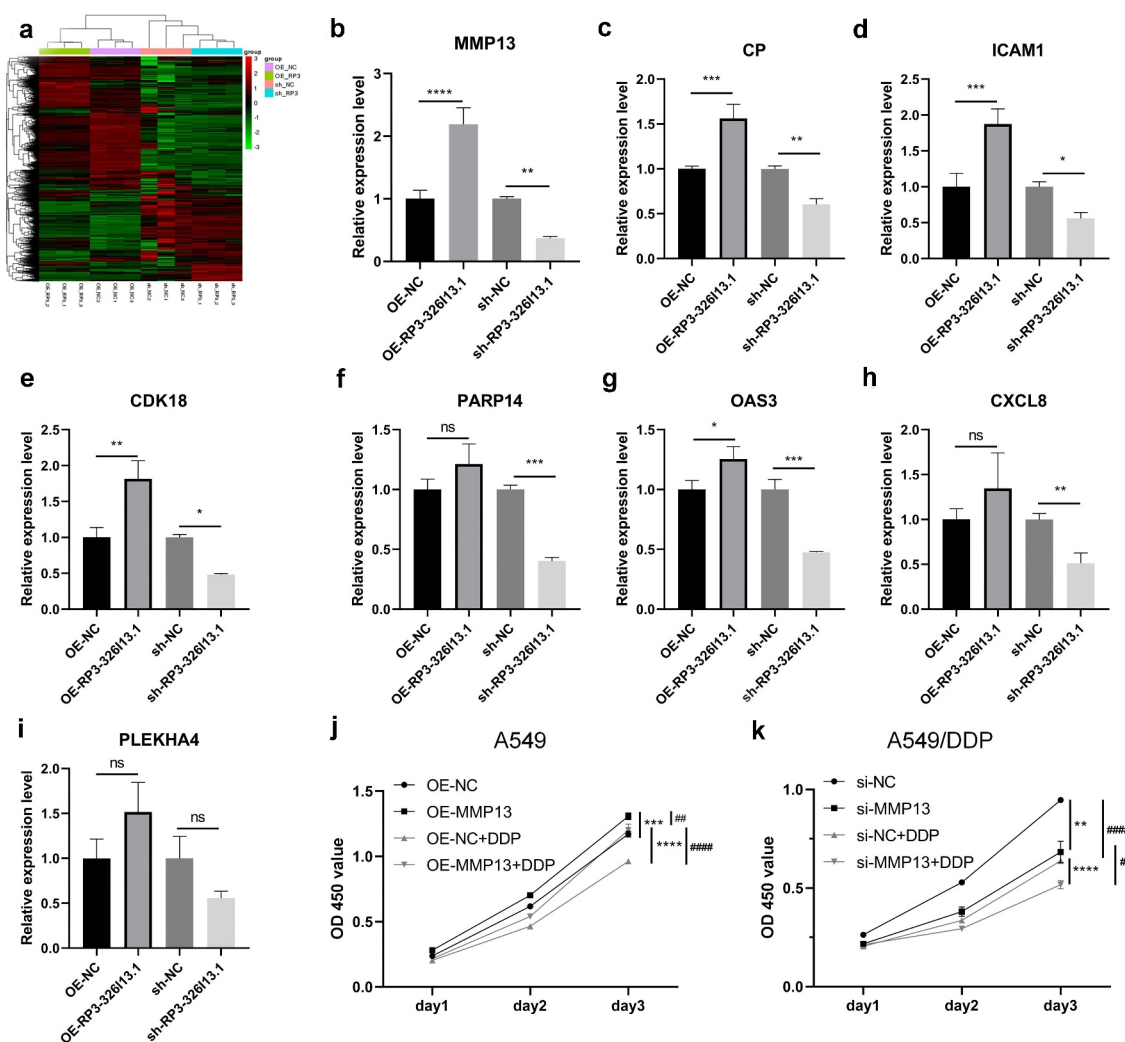


Figure 5. MMP13 served as a downstream mRNA of RP3-326I13.1. (a) The heat map showed the differential mRNA expression in RP3-326I13.1 overexpression and knockdown cells of LAD. (b-i) RT-qPCR was used to verify the differentially expressed mRNA in the sequencing results, including MMP13, CP, ICAM1, CDK18, PARP14, OAS3, CXCL8 and PLEKHA4. (j, k) It showed the proliferation ability of MMP13 overexpression (j) and knockdown (k) with or without DDP treatment by CCK-8 assays. ns: no significance, * $P < 0.05$, ** $P < 0.01$, *** $P < 0.001$, **** $P < 0.0001$.

Studies have shown that MMP13 was involved in DDP resistance [19]; therefore, we further studied the role of MMP13 in DDP-resistance of LAD cell lines. Subsequently, we performed CCK-8 assays, found that MMP13 overexpression promoted the proliferation of A549 cells, and after treatment with DDP, cell proliferation ability was inhibited, but MMP13 overexpression could reverse the inhibitory effect of DDP (Figure 5(j)). MMP13 knockdown inhibited the proliferation of A549/DDP cells, and after treatment with DDP, the proliferation of A549/DDP cells was further inhibited, and in the DDP treatment group, MMP13 knockdown increased the DDP-sensitivity of A549/DDP cells and inhibited the

proliferation ability of A549/DDP cells (Figure 5(k)).

RP3-326I13.1 enhanced DDP-resistance from nude mice experiment cell lines

The size of the tumor formed as shown in Figure 6(a). On the 7d, 14d, 21d, and 28d after tumor formation, the relative tumor volume of each mouse was measured and counted, and the tumor growth curve was drawn (Figure 6(b)). Compared with the 7th day of each group, the volume of tumors on 14th day, 21st day, and 28th day gradually increased. And the tumor growth of the OE-RP3-326I13.1+ DDP group

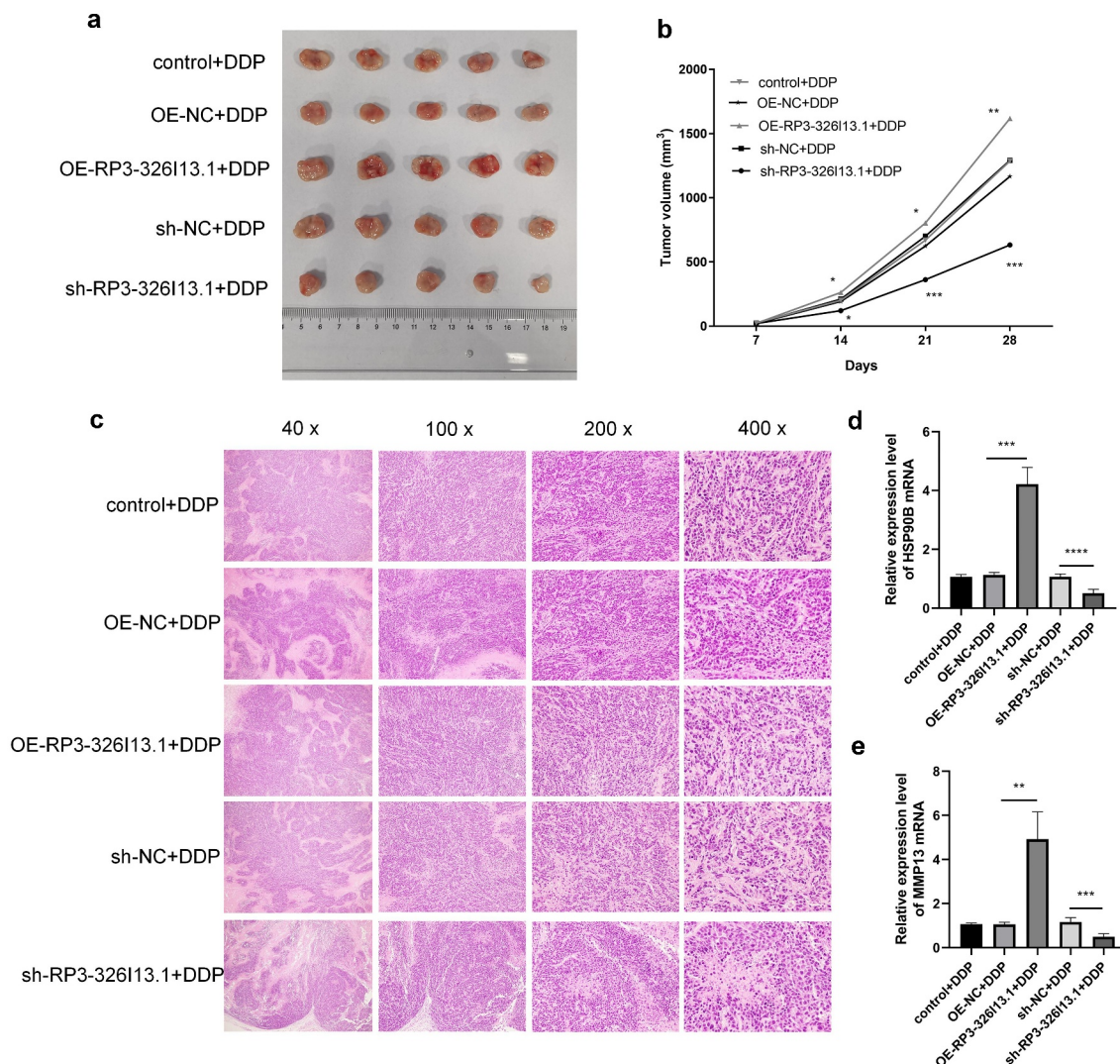


Figure 6. RP3-326I13.1 promoted tumor growth and decreased the sensitivity to cisplatin chemotherapy in nude mice. (a) Representative images of nude mice xenografts after injection of RP3-326I13.1 overexpression or knockdown cells and treatment with DDP (including control+DDP, OE-NC+DDP, OE-RP3-326I13.1+ DDP, sh-NC+DDP, sh-RP3-326I13.1+ DDP) for 28 days. (b) The volume of xenografted tumors in each group of nude mice. The tumor volumes were measured every 7 days (tumor volume = length \times width²/2). (c) Representative images of tumor cell necrosis in xenografted tumors in each group were analyzed by HE staining. (d, e) The mRNA and protein expression levels of HSP90B and MMP13 in the sh-RP3-326I13.1+ DDP group were lower than those in the sh-NC+DDP group, while the mRNA and protein expression levels of HSP90B and MMP13 in the OE-RP3-326I13.1 + DDP group It is higher than the OE-NC+DDP group. * $P < 0.05$, ** $P < 0.01$, *** $P < 0.001$, **** $P < 0.0001$.

on the 14th, 21st and 28th days was significantly higher than the control group. RP3-326I13.1 knockdown had the opposite effect, the tumor growth on the 14th, 21st, and 28th days was significantly lower than the control group. Moreover, hematoxylin-eosin (HE) staining analysis showed that tumor cell necrosis decreased in the OE-RP3-326I13.1+ DDP group compared to the OE-NC+DDP group, and compared with the sh-NC+DDP group, tumor cell necrosis

significantly increased in the sh-RP3-326I13.1 + DDP group (Figure 6(c)).

Next, qPCR was used to detect the mRNA and protein expression levels of HSP90B and MMP13 in tumor tissues of nude mice. The expression levels of HSP90B and MMP13 mRNA and protein level of the sh-RP3-326I13.1+ DDP group were lower than the sh-NC+DDP group, while the mRNA and protein expression levels of HSP90B and MMP13 of the OE-RP3-326I13.1+ DDP group

was higher than the OE-NC+DDP group (Figure 6 (d,e,f)).

Discussion

DDP is a strong nonspecific cell cycle blocking drug, which has cytotoxicity, can inhibit the DNA replication process of cancer cells, and has a strong anti-tumor effect [20]. However, DDP-resistance is increasing severity, and it has become one of the main obstacles in clinical chemotherapy [21,22]. The mechanism of DDP-resistance is extremely complex [23].

Ritu Chaudhary et al. found that RP3-326I13.1 promoted the progression of colorectal cancer by combining with Matrin 3, and targeted deletion of RP3-326I13.1 significantly induced resistance to chemotherapeutics [14]. We found that RP3-326I13.1 was highly expressed in A549/DDP cells. And compared with adjacent tissues and relief tissues, RP3-326I13.1 expression was higher in LAD tissues and progress tissues. These results indicated that RP3-326I13.1 may produce a marked effect in the DDP-resistance of LAD.

By identifying and inhibiting these cancer-promoting molecules, the progression of cancer could not only be inhibited, but also regain the sensitivity to chemotherapy [24]. We found that the up-regulation of RP3-326I13.1 significantly promoted the proliferation, migration, invasion and DDP-resistance of LAD cell lines, while knockdown of RP3-326I13.1 inhibited these effects. DDP-induced cell cycle arrest is one of the keys to exert anti-cancer effect [25]. The cell cycle is an evolutionarily conserved process, including G1, S, G2, and M phases [26]. We found that knockdown of RP3-326I13.1 induced G1 arrest and decreased the proportion of G2 + S phase cells in LAD cell lines, thereby inhibiting LAD cell lines division. These results indicated that knockdown of RP3-326I13.1 could inhibit the proliferation, migration, and invasion of LAD cell lines and gain sensitivity to DDP.

LncRNAs can exert its function by interacting with some specific proteins [27,28]. We identified the differentially expressed HSP90B through RNA pulldown and mass spectrometry. HSP90B is a member of the HSP90 family and a marker located in the endoplasmic reticulum [29,30]. The HSP90

family is involved in regulating cell proliferation, migration, invasion, and DDP-resistance [31-34]. Subsequently, we found that HSP90B could be combined with RP3-326I13.1 and enhance the invasion and proliferation ability while decreasing the apoptosis rate of LAD cell lines, thereby enhancing DDP-resistance. In addition, HSP90B knockdown could reverse the proliferation, invasion, and DDP-resistance induced by RP3-326I13.1.

We further studied the downstream mRNA of RP3-326I13.1 through transcriptome sequencing. QPCR was used to verify the candidate genes and found that MMP13, CP, ICAM1, CDK18, and OAS3 mRNA expression levels had corresponding changing in regulated expression of RP3-326I13.1. Among them, MMP13 has been reported to be involved in the mechanism of DDP-resistance in some tumors [19,35]. Our further studies found that MMP13 could promote the proliferation of LAD cell lines by increasing DDP-resistance.

The xenograft tumor model further verified the effect of RP3-326I13.1 in vivo, and found that the tumor growth of nude mice was the fastest in the OE-RP3-326I13.1+ DDP group, while RP3-326I13.1 knockdown significantly inhibited tumor growth. We also detected the expression levels of HSP90B and MMP13 mRNA in the tumor tissues of five groups of nude mice, and the results were consistent with cell verification. These results suggested that HSP90B and MMP13 synergized with RP3-326I13.1 to promote tumorigenesis and DDP-resistance in nude mouse model of LAD.

In summary, our results demonstrated that RP3-326I13.1 was highly expressed in DDP-resistant cells and tissues of LAD. RP3-326I13.1 could promote the proliferation, invasion, and migration of LAD cell lines by binding to HSP90B and up-regulating MMP13 expression, thus leading to DDP-resistance in LAD. These indicated that RP3-326I13.1 may serve as a therapeutic target and a biomarker for predicting DDP-resistance in LAD.

Materials and methods

Cell culture

The A549 and A549/DDP cells were obtained from the Cell Bank of the Chinese Academy of

Sciences (Beijing, China), and then cultured in Roswell Park Memorial Institute (RPMI)-1640 (Gibco; Thermo Fisher Scientific, Inc. MA, USA) containing 10% fetal bovine serum (FBS) (Gibco; Thermo Fisher Scientific, Inc. MA, USA). A549/DDP cells were treated with 2 $\mu\text{g}/\text{ml}$ DDP (Beyotime Institute of Biotechnology, Shanghai, China) to maintain resistance capability.

Human LAD tissue specimens and DDP-treated LAD specimens

Fifty-seven samples of LAD and paired adjacent tissues were collected from 28 males and 29 females (age range, 23–76 years; mean age, 46.68 ± 16.52) at the First Affiliated Hospital of Wenzhou Medical University between August 2013 and August 2014 (Table 2). After surgical removal of tissue samples, they were frozen and stored in liquid nitrogen within 15 min, and all samples were confirmed by histopathological examination.

Human LAD relief tissues (DDP-sensitive, $n = 25$) and progression tissues (DDP-resistant, $n = 32$) were collected at the First Affiliated Hospital of Wenzhou Medical University between 2010 and 2015 (Table 3). All tissue samples had to meet the following criteria: (1) patients with primary LAD and clinical-stage IIIB-IV; (2) the first-line chemotherapy regimen: DDP 25 mg/m^2 combination with gemcitabine 1000 mg/m^2 or

Table 2. Clinical features between cisplatin-sensitive group and cisplatin-resistant group of lung adenocarcinoma.

Term	Sensitive group ($n = 18$)	Resistant group ($n = 20$)
Sex		
Male	10	11
Female	8	9
TMN stage		
IIIb	11	12
IV	7	8
Histological degree		
Poor	4	5
Moderate	9	10
High	5	5
Lymph node metastasis		
Yes	8	6
No	10	14
Smoking		
Yes	5	6
No	13	14

Table 3. shRNA or siRNA sequences.

Gene		shRNA or siRNA sequences (5'-3')
RP3-326I13.1	shRNA1	GTTCCACTGAAATAGCGAGTAACTCGAGTTA CTCGCTATTTTCAGTGGAATTTTT
	shRNA2	GCAGGATAAACACTTACAAAGACTCGAGTCT TTGTAAGTGTTCCTCTGTTTT
	shRNA3	ATGGCAGG AGCAAGTGGTTAT
	shRNANC	GCTCAACAGAAGCTGAGCAAATCTCGAGATT TGCTCAGCTTCTGTTGAGTTTT
	HSP90B	siRNA1 GAAGGAACGAGAGAAGGAATT siRNA2 GCAGAGGAAGAGAAAGGUGTT siRNA3 AGAGAAAGGUGAGAAAGAATT siRNA4 GAGAAAGAAGAGGAAGAUATT siRNA NC UUCUCCGAACGUGUCACGUTT
MMP13	siRNA1	AGAAAGACUGCAUUUCUCGGA
	siRNA2	AAGAAAGACUGCAUUUCUCGG
	siRNA3	UUUUUCAUGACAUCUAAGGUG
	siRNA NC	UUCUCCGAACGUGUCACGUTT

NC, Negative control; shRNA, short hairpin RNA; siRNA, small interfering RNA.

paclitaxel 80 mg/m^2 for 21 days, with each patient receiving 3 cycles of treatment. Patients were divided into a “DDP-sensitive group” (relief) and a “DDP-resistant group” (progression) based on medical imaging tests, as computed tomography (CT), magnetic resonance imaging (MRI), serum tumor markers, and Response Evaluation Criteria in Solid Tumors (RECIST) criteria [36]. These patients underwent fiberoptic bronchoscopy to obtain lung cancer tissue after receiving three cycles of treatment, which was cryopreserved in liquid nitrogen within 15 minutes, and all specimens were confirmed by histopathological examination.

These study was approved by the Institutional Ethical Review Committee of the First Affiliated Hospital of Wenzhou Medical University (YS2018001) and carried out in strict accordance with the guidelines of the Declaration of Helsinki [37].

Transfection

The overexpression lentiviral vector of RP3-326I13.1 (OE-RP3-326I13.1) and human matrix metalloproteinase-13 (MMP-13) (OE-MMP13) and their corresponding negative control (OE-NC) were purchased from Shanghai GeneChem Co., Ltd. A549 cells were transfected with the lentiviral vector targeting OE-RP3-326I13.1 or OE-MMP13. The interference vector short

Table 4. Sequences of the primers used for RT-qPCR.

Primer ID	Primer sequences (5'-3')
RP3-326I13.1 Forward	TCTTCTGCTGACTTGCCTT
RP3-326I13.1 Reverse	CACCTCCAACATAGGGGATCG
HSP90B Forward	CAAACCTATGTCCGCCGTG
HSP90B Reverse	AGATGTTTCAGG GGCAGATCC
MMP13 Forward	CCAGTTTGCAGAGCGCTACC
MMP13 Reverse	GACTGCATTCTCGGAGCCT
OAS3 Forward	CTTGCCAGCTTCGAAAACC
OAS3 Reverse	TAAAGGAGGGCTGGCATCAC
CP Forward	CCAGCCTGGGCGAAAGAAA
CP Reverse	AGATATTGGAATGTTCCGTGTAAC
ICAM1 Forward	GACCAGAGGTTGAACCCAC
ICAM1 Reverse	GCGCCGAAAGCTGTAGAT
PARP14 Forward	GTGTGCAGAATGCTAAGACCG
PARP14 Reverse	GGAGCTCTGGTCCAGCTTTT
PLEKHA4 Forward	GCCCTCACTTAGGTCTTGGG
PLEKHA4 Reverse	TGGTGTCTTGGACTTGGT
CXCL8 Forward	GCTCTGTGTGAAGGTGCAGTT
CXCL8 Reverse	AATTCTCAGCCCTTTCAAAAACCT
CDK18 Forward	GGTATAAGGAGCAAAGGCCCG
CDK18 Reverse	AAGTTCTCATTCCGCCGGTT
β -actin Forward	CATGTACGTTGCTATC CAGGC
β -actin Reverse	CTCCTTAATGTCACGCACGAT

RT-qPCR, real-time fluorescent quantitative PCR.

hairpin RNAs (shRNAs) targeting RP3-326I13.1 (shRNA-RP3-326I13.1) and the corresponding negative control (sh-NC) were purchased from Shanghai GeneChem Co., Ltd. The interference vector small interfering RNAs (siRNAs) targeting HSP90B and MMP13, as well as their negative control (si-NC) were synthesized by Shanghai GeneChem Co., Ltd. A549/DDP cells were transfected with sh-RP3-326I13.1, si-HSP90B, and si-MMP13, as well as their sh-NC or si-NC. shRNA and siRNA sequences were listed in Table 4. The best shRNA and siRNA sequences were selected as subsequent experimental groups.

Library preparation for transcriptome sequencing and analysis

A total of 1 μ g RNA per sample (including sh-RP3-326I13.1, sh-NC, and OE-RP3-326I13.1, OE-NC) were used as input material for RNA. Sequencing libraries were generated using NEBNext[®] Ultra[™] (New England Biolabs, USA). We screened the differential mRNAs between sh-RP3-326I13.1 vs. sh-NC group and the differential mRNAs between OE-RP3-326I13.1 vs. OE-NC, and then obtain the two common differential mRNAs for PCR verification.

QPCR

Total RNA in tissues and cells was extracted by RNA extraction kit (Thermo Fisher Scientific, Inc. MA, USA). The quality and concentration of RNA were tested by Nano-drop 2000 (Thermo Fisher Scientific, Inc. MA, USA). Gene expression levels were determined by real-time fluorescent quantitative PCR (qPCR) in an ABI 7500 instrument (Thermo Fisher Scientific, Inc. MA, USA). The primer sequences were listed in Table 5. The 20 μ l reaction volume consisted of 6 μ l RNase-free water, 10 μ l SYBR Premix (2 \times), 1 μ l forward primer (10 μ M), 1 μ l reverse primer (10 μ M), and 2 μ l cDNA template. qPCR reaction procedure included a denaturation step of 30 sec at 95 $^{\circ}$ C, 40 cycles (5 sec at 95 $^{\circ}$ C, 30 sec at 60 $^{\circ}$ C). β -actin as the internal reference, and results analysis by the $2^{-\Delta\Delta C_t}$ method.

The half maximal inhibitory concentration (IC50) of DDP assay

3×10^3 cells were plated in 96-well plates and incubated until the cell adhered, and then added DDP containing 0, 1 μ g/ml, 2 μ g/ml, 4 μ g/ml, 6 μ g/ml, 10 μ g/ml, 14 μ g/ml concentration gradient complete medium. After 48 h incubation, 10 μ l of cell counting kit-8 (CKK-8, Dojindo Molecular Technologies, Inc. Kumamoto, Japan) solution was added and incubated for 1 h at 37 $^{\circ}$ C. A microplate

Table 5. Some protein-related information sheet of mass spectrum.

Protein ID	Coverage (%)	Mass (Da)	Unique Peptide	Identified by
sp Q13085 ACACA_HUMAN	46.55	265,551.7	100	Sense
sp P11498 PYC_HUMAN	53.82	129,632.6	74	
sp P08238 HSP90B_HUMAN	51.52	83,263.5	27	
sp P04406 G3P_HUMAN	72.24	36,053	45	
sp P07437 TBB5_HUMAN	68.24	49,670.5	5	
sp Q13085 ACACA_HUMAN	37.68	265,551.7	87	Antisense
sp P11498 PYC_HUMAN	46.26	129,632.6	48	
sp P08238 HSP90B_HUMAN	42.27	83,263.5	19	
sp P14618 KPYM_HUMAN	57.44	57,936.4	28	
sp P07437 TBB5_HUMAN	55.86	49,670.5	7	

reader (Molecular Devices, CA, USA) was used to measure absorbance at 450 nm. Cell viability (%) = $(A_{\text{DDP}} - A_{\text{blank}})/(A_{0 \text{ DDP}} - A_{\text{blank}}) \times 100\%$. IC50 of DDP was calculated by the probit regression model in SPSS software (v22.0; IBM Corp.USA).

CCK-8 assay

3×10^3 cells/well were added in 96-well plates, after the cells adhered, changed the cell solution, and added the corresponding concentration of DDP to the DDP group. The concentration of A549 cells treated with DDP was 1 $\mu\text{g/ml}$, and A549/DDP cells treated with DDP was 2 $\mu\text{g/ml}$. At each time point, 10 μl of CCK-8 solution was added and incubated for 1 h at 37°C, repeated for 3 days. A microplate reader (Tecan, German) was used to measure absorbance at 450 nm.

Colony formation assay

500 cells/well were inoculated in six-well plate, after 14 days of incubation, cells were fixed in methanol for 20 min and stained with crystal violet (Beyotime Institute of Biotechnology, Shanghai, China) for 30 min at room temperature. The standard was to use more than 50 cell clusters as a cell clone. The number of cell clones was evaluated to determine the ability of cell clone formation.

Cell migration experiment

Logarithmic growth cells were collected and plated into six-well plates. When cells density reached 90%, a 200 μl pipette tip was used to make scars on the cells. Phosphate buffer saline (PBS, Gibco; Thermo Fisher Scientific, Inc. MA, USA) was used to wash and remove floating cells and incubated with a serum-free RPMI-1640 medium to reduce the influence of cell proliferation. An inverted microscope (Olympus Corporation, Japan) was used to capture scratch images at a magnification of 10 \times at 0 h and 48 h.

Cell invasion assay

Transwell pore polycarbonate membrane insert (24-wells, Corning, pore size 8 μm , New York,

USA) was used, and a layer of Matrigel (BD Biocoat, Corning, New York, USA) was coated on the insert. The upper chamber was inoculated with 1×10^4 cells, and the lower chamber used RPMI-1640 medium containing 20% FBS. After 48 h incubation, cells were fixed and stained. Pictures were taken under the microscope (Olympus Corporation, Japan).

Cell apoptosis assay

PBS was used to wash the cells twice, and cells were added 300 μl binding buffer and 50 μl 1 \times Annexin, and incubated at room temperature for 15 min, and added 5 μl of propidium Iodide (PI) staining 5 min before being tested on a flow cytometer (Beckman Coulter, Inc. Indianapolis, USA). The parameters are 488 nm excitation light wavelength, 515 nm bandpass filter for fluorescence detection, and another filter with a wavelength greater than 560 nm for PI detection. FlowJo software was used for data processing and analysis.

Cell cycle assay

The collected cells were mixed with 3 ml PBS, centrifugated at 1000 g for 5 min, and added 5 ml 75% ethanol to the collected cell pellet, incubated at 4°C in the dark for more than 18 hours. The collected cells were added 500 μl PI/RNase staining solution and incubated for 15 min at room temperature in the dark. Finally, it was tested on a flow cytometer (Beckman Coulter, Inc. Indianapolis, USA). FlowJo software (Becton, Dickinson & Company, Ashland, USA) was used for data processing and analysis.

In vivo xenograft assay

BALB/c, male nude mice, 4-week-old, weighing 18–20 g (Shanghai Slaughter Laboratory Animal Co., China) were housed in an environment with a temperature of $22 \pm 1^\circ\text{C}$, relative humidity of $50 \pm 1\%$, and a light/dark cycle of 12/12 h. All animal studies (including the mice euthanasia procedure) were done in compliance with the regulations and guidelines of Wenzhou Medical University institutional animal care

(WYDW2020-0380), the ARRIVE guidelines [38] and the National Institutes of Health guide for the care and use of laboratory animals.

Experimental steps: Nude mice were divided into five groups ($n = 5/\text{group}$): control+DDP, OE-NC+DDP, OE-RP3-326I13.1+ DDP, sh-NC+DDP and sh-RP3-326I13.1+ DDP. According to experimental groups, 1×10^6 LAD cell lines were injected into nude mice. After 1 week, DDP was injected into the tail vein of the nude mice at a dose of 5 mg/kg/mouse. The relative size of the tumor was measured and counted at 7, 14, 21 and 28 days after tumorigenesis [tumor volume = (length \times width²)/2]. Subsequently, the mice were euthanized by cervical dislocation, and tumors were collected and photographed under low temperature conditions. A part of the obtained tumors prepared as paraffin blocks were stained with hematoxylin-eosin (HE) and photographed; the other part was subjected for RNA extraction to detect the mRNA expression levels of HSP90B and MMP13.

RNA pulldown and mass spectrometry

The basic principle is to first design the sense and antisense strand PCR primers, and form the sense and antisense strands of RP3-326I13.1 by PCR to obtain the DNA template with absorbing ability. Further, RP3-326I13.1 is labeled with biotin, and then some of its complexes can be formed with RP3-326I13.1 to form RP3-326I13.1-RBP complexes and obtain the RBP. The RNA pull-down kit (Thermo Fisher Scientific, Inc. MA, USA) was used to adsorb proteins that interacted with RP3-326I13.1. Probe RP3-326I13.1 was labeled and collected the eluent containing specifically bound proteins, and detected the enriched proteins by sodiumdodecylsulfate-polyacrylamide gel electrophoresis (SDS-PAGE) electrophoresis silver staining, and identified the differential proteins by mass spectrometry.

Statistical analysis

The student's t-test was used for comparison between two groups for normally distributed data, and the Mann-Whitney U-test was used for

non-normally distributed data. Statistical analysis was performed using SPSS software (v22.0; IBM Corp. USA) and GraphPad Prism (v8.0; GraphPad Software, Inc. USA) was used to generate graphs. $P < 0.05$ was considered statistically significant. Data were expressed as the mean \pm standard deviation of three independent tests.

Disclosure statement

No potential conflict of interest was reported by the author(s).

Funding

This work was supported by Zhejiang Provincial Natural Science Foundation [grant no. LY19H200002], the National Natural Science Foundation of China [grant no. 81672088], the Wenzhou Municipal Science and Technology Bureau of China [grant no. Y20190461] and Zhejiang Provincial Research Center for Cancer Intelligent Diagnosis and Molecular Technology [grant no. JBZX-202003].

Availability of data and materials

Requests for data, resources, and reagents should be directed to the corresponding author Yumin Wang (wangyumin0577@wmu.edu.cn).

Ethics approval and consent to participate

This study involving human participants was approved by the Institutional Ethical Review Committee of the First Affiliated Hospital of Wenzhou Medical University (YS2018001) and carried out in strict accordance with the guidelines of the Declaration of Helsinki. All animal studies were performed in compliance with the regulations and guidelines of Wenzhou Medical University institutional animal care (WYDW2020-0380), the ARRIVE guidelines and the National Institutes of Health guide for the care and use of laboratory animals.

Authors contributions

HZ designed experiments. HZ, XH, and WS conducted experiments. SX and JC contributed to data analysis. HZ, XH, and WS wrote and revised the manuscript. KH and YW supervised the research and revised the manuscript. KH and YW confirmed the authenticity of all the raw data. All authors have read and agreed to the final version of the manuscript.

References

- [1] Han Y, Ma Y, Wu Z, et al. Histologic subtype classification of non-small cell lung cancer using PET/CT images. *Eur J Nucl Med Mol Imaging*. 2021;48:350–360.
- [2] Arriagada R, Auquier A, Burdett S, et al.; Group NMA-C. Adjuvant chemotherapy, with or without post-operative radiotherapy, in operable non-small-cell lung cancer: two meta-analyses of individual patient data. *Lancet*. 2010;375:1267–1277.
- [3] Fathi AT, Brahmer JR. Chemotherapy for advanced stage non-small cell lung cancer. *Semin Thorac Cardiovasc Surg*. 2008;20:210–216.
- [4] Nagasaka M, Gadgeel SM. Role of chemotherapy and targeted therapy in early-stage non-small cell lung cancer. *Expert Rev Anticancer Ther*. 2018;18:63–70.
- [5] Kibria G, Hatakeyama H, Harashima H. Cancer multi-drug resistance: mechanisms involved and strategies for circumvention using a drug delivery system. *Arch Pharm Res*. 2014;37:4–15.
- [6] Qu Y, Tan HY, Chan YT, et al. The functional role of long noncoding RNA in resistance to anticancer treatment. *Ther Adv Med Oncol*. 2020;12:1758835920927850.
- [7] Galluzzi L, Senovilla L, Vitale I, et al. Molecular mechanisms of cisplatin resistance. *Oncogene*. 2012;31:1869–1883.
- [8] Kuo CC, Hanzelmann S, Senturk Cetin N, et al. Detection of RNA-DNA binding sites in long noncoding RNAs. *Nucleic Acids Res*. 2019;47:e32.
- [9] Kim T, Croce CM. Long noncoding RNAs: undeciphered cellular codes encrypting keys of colorectal cancer pathogenesis. *Cancer Lett*. 2018;417:89–95.
- [10] Xu H, Brown AN, Waddell NJ, et al. Role of long noncoding RNA Gas5 in cocaine action. *Biol Psychiatry*. 2020;88:758–766.
- [11] Ming H, Li B, Zhou L, et al. Long non-coding RNAs and cancer metastasis: molecular basis and therapeutic implications. *Biochim Biophys Acta Rev Cancer*. 2021;1875:188519.
- [12] Chi HC, Tsai CY, Tsai MM, et al. Roles of long noncoding RNAs in recurrence and metastasis of radiotherapy-resistant cancer stem cells. *Int J Mol Sci*. 2017;18. DOI:10.3390/ijms18091903
- [13] Zhou C, Duan S. The role of long non-coding RNA NNT-AS1 in neoplastic disease. *Cancers (Basel)*. 2020;12. DOI:10.3390/cancers12113086
- [14] Chaudhary R, Gryder B, Woods WS, et al. Prosurvival long noncoding RNA PINCR regulates a subset of p53 targets in human colorectal cancer cells by binding to Matr3n. *Elife*. 2017;6. DOI:10.7554/eLife.23244.
- [15] Schopf FH, Biebl MM, Buchner J. The HSP90 chaperone machinery. *Nat Rev Mol Cell Biol*. 2017;18:345–360.
- [16] Li J, Buchner J. Structure, function and regulation of the hsp90 machinery. *Biomed J*. 2013;36:106–117.
- [17] Pan C, Chun J, Li D, et al. Hsp90B enhances MAST1-mediated cisplatin resistance by protecting MAST1 from proteosomal degradation. *J Clin Invest*. 2019;129:4110–4123.
- [18] Muppurala UK, Honavar VG, Dobbs D. Predicting RNA-protein interactions using only sequence information. *BMC Bioinformatics*. 2011;12:489.
- [19] Ansell A, Jerhammar F, Ceder R, et al. Matrix metalloproteinase-7 and -13 expression associate to cisplatin resistance in head and neck cancer cell lines. *Oral Oncol*. 2009;45:866–871.
- [20] Zhu S, Pabla N, Tang C, et al. DNA damage response in cisplatin-induced nephrotoxicity. *Arch Toxicol*. 2015;89:2197–2205.
- [21] Schiller JH, Harrington D, Belani CP, et al. Comparison of four chemotherapy regimens for advanced non-small-cell lung cancer. *N Engl J Med*. 2002;346:92–98.
- [22] Eljack ND, Ma HY, Drucker J, et al. Mechanisms of cell uptake and toxicity of the anticancer drug cisplatin. *Metallomics*. 2014;6:2126–2133.
- [23] Chen SH, Chang JY. New insights into mechanisms of cisplatin resistance: from tumor cell to microenvironment. *Int J Mol Sci*. 2019;20:4136.
- [24] Mirzaei S, Gholami MH, Hashemi F, et al. Employing siRNA tool and its delivery platforms in suppressing cisplatin resistance: approaching to a new era of cancer chemotherapy. *Life Sci*. 2021;277:119430.
- [25] Lv M, Zhuang X, Zhang Q, et al. Acetyl-11-keto-beta-boswellic acid enhances the cisplatin sensitivity of non-small cell lung cancer cells through cell cycle arrest, apoptosis induction, and autophagy suppression via p21-dependent signaling pathway. *Cell Biol Toxicol*. 2021;37:209–228.
- [26] Guo H, Deng H, Liu H, et al. Nickel carcinogenesis mechanism: cell cycle dysregulation. *Environ Sci Pollut Res Int*. 2021;28:4893–4901.
- [27] Wang KC, Yang YW, Liu B, et al. A long noncoding RNA maintains active chromatin to coordinate homeotic gene expression. *Nature*. 2011;472:120–124.
- [28] Jjd H, Man JHS, Schatz JH, et al. Translational remodeling by RNA-binding proteins and noncoding RNAs. *Wiley Interdiscip Rev RNA*. 2021;12:e1647.
- [29] Chen B, Piel WH, Gui L, et al. The HSP90 family of genes in the human genome: insights into their divergence and evolution. *Genomics*. 2005;86:627–637.
- [30] Pugliese L, Georg RC, Fietto LG, et al. Expression of genes encoding cytosolic and endoplasmic reticulum HSP90 proteins in the aquatic fungus *Blastocladiella emersonii*. *Gene*. 2008;411:59–68.
- [31] Wu J, Liu T, Rios Z, et al. Heat shock proteins and cancer. *Trends Pharmacol Sci*. 2017;38:226–256.
- [32] Chatterjee S, Burns TF. Targeting heat shock proteins in cancer: a promising therapeutic approach. *Int J Mol Sci*. 2017;18. DOI:10.3390/ijms18091978
- [33] Nagaraju GP, Long TE, Park W, et al. Heat shock protein 90 promotes epithelial to mesenchymal

- transition, invasion, and migration in colorectal cancer. *Mol Carcinog.* [2015](#);54:1147–1158.
- [34] Mortensen ACL, Mohajershojai T, Hariri M, et al. Overcoming limitations of cisplatin therapy by additional treatment with the HSP90 inhibitor onalespib. *Front Oncol.* [2020](#);10:532285.
- [35] Kaplancikli ZA, Altintop MD, Atli O, et al. Synthesis and evaluation of a new series of thiazole derivatives as potential antitumor agents and MMP inhibitors. *Anticancer Agents Med Chem.* [2017](#);17:674–681.
- [36] Wahl RL, Jacene H, Kasamon Y, et al. From RECIST to PERCIST: evolving considerations for PET response criteria in solid tumors. *J Nucl Med.* [2009](#);50(Suppl 1):122S–50S.
- [37] World Medical A. World medical association declaration of Helsinki: ethical principles for medical research involving human subjects. *JAMA.* [2013](#);310:2191–2194.
- [38] Percie du Sert N, Ahluwalia A, Alam S, et al. Reporting animal research: explanation and elaboration for the ARRIVE guidelines 2.0. *PLoS Biol.* [2020](#);18:e3000411.